Current Research in Food Science 8 (2024) 100767

Contents lists available at ScienceDirect

Current Research in Food Science

journal homepage: www.sciencedirect.com/journal/current-research-in-food-science

Effect of brewer's spent grain melanoidins on Maillard reaction products during storage of whey protein model systems

Slim Blidi [a], Antonio Dario Troise [b], Mattia Zazzaroni [a], Sabrina De Pascale [b], Sarah Cottin [a], Keith Sturrock [c], Andrea Scaloni [b], Alberto Fiore [a,*]

[a] School of Applied Sciences, Division of Engineering and Food Science, University of Abertay, Bell Street, DD1 1HG, Dundee, Scotland, United Kingdom
[b] Proteomics, Metabolomics & Mass Spectrometry Laboratory, Institute for the Animal Production System in the Mediterranean Environment, National Research Council, 80055 Portici, Italy
[c] School of Applied Sciences, Division of Psychology and Forensic Science, University of Abertay, Bell Street, DD1 1HG, Dundee, Scotland, United Kingdom

ARTICLE INFO

Handling Editor: Professor Aiqian Ye

Keywords:
Maillard reaction
Glycation compounds
α-dicarbonyl compounds
Melanoidins
Whey proteins
Dairy products

ABSTRACT

Maillard reaction readily takes place in dairy products because of the association between thermal treatments, extended storage and the matrix composition. Along with the impairment of protein digestion, the formation of glycation and α-dicarbonyl compounds is a concern for quality attributes of whey proteins when used as ingredients. In this paper, we outline the capacity of brewer's spent grain melanoidins in reducing the accumulation of α-dicarbonyl compounds, thus controlling the formation of dietary advanced glycation end-products in accelerated shelf life at 35 °C. Results revealed that brewer's spent grain melanoidins targeted methylglyoxal and glyoxal reactivity leading to the reduction of *N*-ε-carboxymethyllysine and methylglyoxal-hydroimidazolone up to 27 and 60%, respectively. We here describe that the presence of melanoidins is instrumental in limiting the undesired effects of α-dicarbonyl compounds on whey proteins.

1. Introduction

Milk proteins consist mainly of caseins and whey proteins (WP), accounting for approximately 80 and 20% of the milk total protein content, respectively (Walstra et al., 2005), while lactose and other reducing sugars can be present up to 7% (Jenness, 1979). WP are extensively used as a food ingredient given their nutritional value and functional attributes. Nevertheless, as for milk, WP are prone to chemical modifications due to processing (Mehta and Deeth, 2016; Karlsson et al., 2019), thus resulting in higher non-canonical amino acids concentration in comparison to caseins (Pischetsrieder and Henle, 2012).

Maillard reaction (MR) involves a cascade of diverse chemical reactions leading to the formation of a broad range of glycation compounds. Besides the classification of reaction pathways within compartmentalized degradation and interaction pools (Yaylayan, 1997), the two most studied chemical classes part of MR products encompass α-dicarbonyl compounds (DCs) and dietary advanced glycation end-products (d-AGEs) (Hellwig and Henle, 2014). DCs include methylglyoxal (MGO) and glyoxal (GO) that, along with other compounds, are generated during caramelisation and the intermediate stages of the MR; both are highly reactive species with a strong affinity for amino groups of peptides and proteins, guanidino moiety of arginine, lysine ε-amino group or the thiol group present in cysteine residues, inducing the formation of a heterogeneous group of polymerizations products. Within d-AGEs, *N*-ε-carboxyethyllysine (CEL), *N*-ε-carboxymethyllysine (CML) and methylglyoxal-hydroimidazolone (MG-H1) are generally regarded as markers to monitor the impact of the MR; their occurrence during food thermal treatment and under storage is a prominent factor in the decline of protein digestibility, reducing essential amino acids bioavailability (Zhao et al., 2017; Zenker et al., 2020).

The contribution of d-AGEs and DCs to the pathophysiological consequences of glycation compounds *in vivo* is still ambiguous as various conclusions were hypothesized for the different d-AGEs (Delgado-Andrade and Fogliano, 2018). Numerous studies recommended lowering the levels of both classes during thermal treatment of foods and storage along with the necessity of the rigorous distinction between protein-bound and free d-AGEs as most of d-AGEs are in the bound form (van Boekel et al., 2010; Zhao et al., 2019).

Among the multitude of technological approaches to control the MR, the role of polyphenols from various plant origins has recently gained growing interest in dairy products because of their naturalness;

* Corresponding author.
E-mail address: a.fiore@abertay.ac.uk (A. Fiore).

https://doi.org/10.1016/j.crfs.2024.100767
Received 14 December 2023; Received in revised form 4 May 2024; Accepted 7 May 2024
Available online 8 May 2024

Abbreviations

2-MQX	2 -methylquinoxaline
ABTS	2,2′-azino-bis (3-ethylbenzothiazoline-6-sulfonic acid)
AG	Aminoguanidine
ANOVA	Analysis of variance
BSG	Brewer's spent grain
BSGM	Brewer's spent grain melanoidins
CEL	*N*-ε-carboxyethyllysine
CML	*N*-ε-carboxymethyllysine
d-AGEs	Dietary advanced glycation end products
DCs	α-dicarbonyl compounds
dw	Dry weight
EDTA	Ethylenediaminetetracetic acid
FRAP	Ferric reducing antioxidant power
GAE	Gallic acid equivalents
GO	Glyoxal
HILIC	Hydrophilic interaction liquid chromatography
HPLC	High-performance liquid chromatography
HR BSGM	Highly roasted brewer's spent grain melanoidins
IR BSGM	Intermediate roasted brewer's spent grain melanoidins
LR BSGM	Low roasted brewer's spent grain melanoidins
MG-H1	Methylglyoxal-hydroimidazolone 1
MG-H3	Methylglyoxal-hydroimidazolone 3
MGO	Methylglyoxal
MR	Maillard reaction
OPA	*o*-phthaldialdehyde
OPD	*o*-phenylenediamine
PVDF	Polyvinylidene fluoride
QX	1-quinoxaline
TEAC	Trolox equivalent antioxidant capacity
TPC	Total phenolic content
TPTZ	2,4,6-Tris(2-pyridyl)-s-triazine
Trolox	6-hydroxy-2,5,7,8-tetramethylchroman-2-carboxylic acid
WP	Whey proteins

consequently, they are sought more as functional food ingredients than synthetic compounds (Lund and Ray, 2017). Besides the use of antioxidant extracts, food functionality can be further promoted via the addition of macromolecules generated during food thermal treatment such as melanoidins. Melanoidins are high-molecular-weight polymers formed in the late stages of the MR from reducing sugars/polysaccharides and proteins/amino acids during food processing and preservation (Román et al., 2017). During melanoidins formation, more diversified and complex pathways occur including polymerization mechanisms usually not included in AGEs formation (Bork et al., 2024). Severe thermal treatments such as roasting cocoa, coffee beans and nuts are the main thermal processes promoting melanoidin formation (Morales et al., 2012). Various studies demonstrated the functional and health properties of melanoidins, which play the role of an antioxidant dietary fiber in food systems (Mesías and Delgado-Andrade, 2017) and can modulate energy intake by controlling the gut-brain response (Walker et al., 2020). Furthermore, recent findings reported the ability of cocoa and coffee melanoidins to scavenge DCs under simulated physiological conditions and in a dairy mimicking system (H. Zhang et al., 2019; Zhang et al., 2021). The scavenging activity can be controlled through the modification of the melanoidin chemical composition, and more specifically enhancing the reactivity of melanoidin-bound polyphenols, by changing roasting parameters (the combination temperature/time) (Blidi et al., 2023).

In this study, melanoidins formed upon roasting of brewer's spent grain (BSG), a widely available yet underutilized by-product of the brewing industry, were investigated for their inhibitory effect on DCs (GO and MGO), protein-bound lysine Amadori compound (quantified through furosine) and d-AGEs (CEL, CML and MG-H1/H3) in WP/glucose and WP/DCs models under experimental storage conditions for up to 14 days. Furthermore, potential mechanisms supporting the aforementioned effects were also explored. Assuming that the interaction among amino acids and sugar is almost unavoidable, we described how polymerization products arising from a vegetable source hence rich of antioxidant and functional polyphenols can be instrumental to the control of advanced products formation in a milk WP model system.

2. Materials and methods

2.1. Chemicals and reagents

GO aqueous solution (40%), MGO aqueous solution (40%), *o*-phenylenediamine (OPD), *o*-phthaldialdehyde (OPA), ethylenediaminetetracetic acid (EDTA), gallic acid, 2,2′-azino-bis (3-ethylbenzothiazoline-6-sulfonic acid) (ABTS) diammonium salt, 2,4,6-tris(2-pyridyl)-s-triazine (TPTZ), aminoguanidine (AG) hydrochloride, glucose, L-serine, sodium azide, acetic acid and formic acid were purchased from Sigma-Aldrich (St. Louis, MO). Hydrochloric acid (HCl, 37%), methanol HPLC-grade, acetonitrile HPLC- and LC-MS-grades, ammonium formate LC-MS-grade, 6-hydroxy-2,5,7,8-tetramethylchroman-2-carboxylic acid (Trolox) and potassium persulfate were obtained from Thermo Fisher Scientific (Waltham, MA). Sodium dihydrogen phosphate dihydrate ($NaH_2PO_4{\cdot}2H_2O$), di-sodium hydrogen phosphate dihydrate ($Na_2HPO_4{\cdot}2H_2O$), sodium acetate, Folin-Ciocalteu′s phenol reagent and iron (III) chloride hexaydrate ($FeCl_3$ $6H_2O$) were acquired from Merck (Darmstadt, Germany). Analytical standards *N*-ε-carboxyethyllysine (CEL) and *N*-ε-carboxyethyllysine-d4 (CEL-d4), *N*-ε-carboxymethyllysine (CML), *N*-ε-carboxymethyllysine-d4 (CML-d4), methylglyoxal hydroimidazolone trifluoroacetic acid salt (MG-H1), methylglyoxal-hydroimidazolone-d3 (MG-H1-d3) and furosine were purchased from Iris Biotech GmbH (Marktredwitz, Germany).

2.2. BSG samples and preparation of brewer's spent grain melanoidins

BSG originating from the *Concerto* barley variety were provided by Lindores Abbey Distillery in Fife, Scotland. The fresh BSG was dried overnight at 60 °C using a convection oven (Memmert, Schwabach, Germany), and then stored in an air-tight container before further use. BSG was roasted in a convection oven (Memmert) according to three different roasting regimes increasing in intensity based on our previous results obtained in the response surface methodology experiment (Blidi et al., 2023): *i*) low roasting at 160 °C, for 60 min; *ii*) intermediate roasting at 185 °C, for 60 min; *iii*) high roasting at 210 °C, for 60 min. Brewer's spent grain melanoidins (BSGM) were obtained according to the method described by Blidi et al. (2023). In brief, roasted BSG was ground using a ring sieve of 0.5 mm in diameter fitted to an electric mill (ZM 200, Retsch, Haan, Germany). Roasted BSG powder (100 g) was extracted in water (1.2 L) for 20 min at 80 °C, with stirring. The supernatant was filtered under vacuum (Whatman 595, Billerica, MA). The filtrate was dialyzed (MW cut-off 14 kDa, D9402, Sigma-Aldrich) at 4 °C, until conductivity was ≤2 μS/cm, as measured by a conductivity meter (DiST 3, Hanna Instruments, Woonsocket, RI) (water renewed at rate of 1 L per cycle) allowing the removal of any potential remaining free sugars, amino acids, and polypeptides (made of up to 140 amino acids). Retentates were then freeze-dried until constant weight was obtained. Dry samples were then stored at −20 °C until further use.

2.3. Determination of total phenolic content and antioxidant activity of the different BSGM types

Prior to analysis, low roasted BSGM (LR BSGM), intermediate roasted BSGM (IR BSGM) and highly roasted BSGM (HR BSGM) were subjected to acidic hydrolysis for the release of bound polyphenols, according to the method used by Oracz et al. (2019) with modifications. In brief, 1.0 mL of 10 M HCl was added to BSGM solution (2.5 mL, 20 mg/mL in 50% aqueous methanol) and heated at 75 °C, for 150 min. After hydrolysis, 1.25 mL of 8 M NaOH was added to neutralize the solution yielding a final volume of 4.75 mL, and the resulting solution was subsequently centrifuged at 4500*g* for 8 min, at 4 °C. The supernatant was filtered using a 0.22 μm polyvinylidene fluoride (PVDF) filter to yield acid-hydrolyzed BSGM. A control sample was prepared as follows: 50 mg of non-treated BSGM was dissolved in 4.75 mL of water and then centrifuged (4500*g* for 8 min, at 4 °C). The supernatant was then filtered using a 0.22 μm PVDF filter.

2.3.1. Determination of total phenolic content of the different BSGM types

The determination of the total phenolic content (TPC) of the three different types of BSGM was carried out following the method described by Blidi et al. (2023). An external calibration curve was constructed using aqueous gallic acid standard solutions ranging in concentrations from 10 to 200 μg/mL. The TPC of the samples was expressed as gallic acid equivalents (GAE) in mg per 100 g of dry weight (mg GAE/100 g dw). All samples were analyzed in triplicate.

2.3.2. Determination of the antioxidant activity of the different BSGM types

2.3.2.1. ABTS radical scavenging activity assay. The antioxidant activity of the three types of BSGM was determined based on the ABTS assay as described by Blidi et al. (2023) Aqueous solutions of Trolox at concentration values ranging between 10 and 250 μM were used for calibration. Results were expressed as Trolox equivalent antioxidant capacity (TEAC) in mg per 100 g of dw (mg TEAC/100 g dw). All measurements were performed in triplicate.

2.3.2.2. Ferric reducing antioxidant power assay of the different BSGM types. The method is adapted from the work of Benzie and Strain (1996). The ferric reducing antioxidant power (FRAP) reagent was prepared fresh each day by mixing 25 mL of 300 mM sodium acetate, pH 3.6, with 2.5 mL of 10 mM TPTZ solution in 40 mM HCl, and 2.5 mL of 20 mM Fe III aqueous solution. 900 μL of FRAP reagent and 100 μL of hydrolysate (initially prepared at a concentration of 40 mg melanoidins/mL) were mixed, and the absorbance at 593 nm of the reaction mixture was measured after 4 min (Thermo Scientific Genesys 10S UV–Vis Spectrophotometer, Waltham, MA). GA was used for external calibration in the range 25–250 μM. Results were expressed in mg GAE/100 g dw.

2.4. Amino groups quantification and sample preparation for the analysis of DCs

To investigate the potential reaction between amino groups and DCs, the amino group content in the three types of BSGM pre- and post-incubation with DCs was evaluated using the OPA assay. In brief, three BSGM solutions (LR, IR and HR BSGM) (10 mg/mL), MGO (6.4 mM) and GO (6.4 mM) were prepared in phosphate buffer (0.1 M, pH 7.0). In brief, 240 μL of MGO/GO solution or phosphate buffer (for the negative control) was added to 240 μL of each melanoidin solution and 720 μL of phosphate buffer. Samples were then incubated for 2, 7 and 14 days, at 35 °C. Once the specific incubation elapsed, the remaining DCs were quantified by adding 200 μL of 0.2% w/v OPD solution containing EDTA (9.6 mmol/L) to 1 mL of sample to derivatize GO and MGO into 1-quinoxaline (QX) and 2 -methylquinoxaline (2-MQX), respectively, as previously described (H. Zhang et al., 2019). After vortexing for 5 s, samples were kept in the dark for 2 h, at 37 °C. After filtering through 0.22 μm PVDF filters, samples were subjected to high-performance liquid chromatography (HPLC) analysis as described in section 2.8. The OPA assay was conducted on the remaining samples based on a prior method (Nielsen et al., 2001). Briefly, 200 μL of each sample was mixed with 1500 μL of freshly prepared OPA reagent. After incubation at room temperature for 2 min, a UV–Vis spectrophotometer (Thermo Scientific Genesys 10S, Waltham, MA) was used to measure the absorbance at 340 nm. An external calibration curve was constructed using standard solutions of L-serine (in the range of 10–150 mg/L) following the incubation conditions previously described.

2.5. Effect of the different BSGM types on the formation of MGO and GO from glucose

The experimental procedure was adapted from a previous method as described by Zhang et al. (2021), with minor modifications. Briefly, 1050 μL of phosphate buffer (control sample) or 350 μL of phosphate buffer plus 700 μL of IR BSGM solution (10 mg/mL) were mixed with 700 μL of glucose (1 M in phosphate buffer, pH 7.0, 0.04% sodium azide). Prepared samples were then incubated for 2, 7 and 14 days at 35 °C. The samples were then derivatized as described in the previous paragraph.

2.6. Quantification of quinoxaline derivatives by HPLC-UV detection

Prior to HPLC analysis, the WP model system samples were prepared according to the method of Prestel et al. (2020) with some modifications. For protein precipitation, each sample (500 μL) was mixed with 100 μL of methanol and incubated at room temperature on an orbital shaker (Thermomixer Comfort, Eppendorf, Hamburg, Germany) at 500 rpm, for 15 min. Samples were subsequently centrifuged at 10 000*g* for 20 min and the supernatant was collected. Derivatization of samples was performed as described in paragraph 2.4.

The quantification of quinoxaline derivatives in all samples was conducted according to the method of Ledbetter et al. (2021) with modifications. The HPLC system consisted of a PerkinElmer Flexar LC pump (Waltham, MA), coupled with a PerkinElmer Flexar diode array detector, and a PerkinElmer Flexar Dionex autosampler (Waltham, MA). Chromatographic separation was carried out onto a 2.7 μm Restek Raptor C18 column (150 mm × 2.1 mm) (Bellefonte, PA), thermostated at 40 °C, at a flow rate of 0.4 mL/min; the injection volume was 20 μL. A binary solvent system gradient of 0.1% v/v formic acid in water (A) and 0.1% v/v formic acid in acetonitrile (B) was used as follows (minutes/% B): (0/2), (2/2), (4/20), (6/20), (14/95), (16/2), (18/2). Chromatograms were recorded at 315 nm. QX and 2-MQX were eluted at 12.42 and 13.69, min, respectively. Peaks identification was achieved by comparing the retention times with those of the standards. External calibration curves were constructed to quantify QX and 2-MQX in the ranges (0.06–3 μg/mL) and (0.06–4 μg/mL), respectively. Limit of detection was 0.006 and 0.009 μg/mL for QX and 2-MQX, respectively, while the limit of quantification was 0.018 and 0.027 μg/mL for QX and 2-MQX, respectively.

Percentage decrease in each DC was calculated using equation (1):

$$\text{Trapping capacity (\%)} = [(\text{amount of DC in control} - \text{amount of DC in sample})/ \text{amount of DC in control}] \times 100 \quad (1)$$

2.7. Effect of the different BSGM types on the formation of d-AGEs and furosine in the WP/MGO, WP/GO and WP/glucose reaction models

WP and glucose concentrations in the studied model systems were calculated according to the protein and carbohydrate concentration ranges in chocolate milk (3.2–3.6% and 5%–9%, respectively) (Roy,

2008). In brief, the three roasted BSGM (LR, IR and HR BSGM, 10 mg/mL), AG (positive control, 6.4 mM), WP (35 mg/mL), glucose (1 M), MGO (6.4 mM) and GO (6.4 mM) were dissolved in phosphate buffer (100 mM, pH 7.0). MGO/GO/glucose solutions (700 μL) were added to WP solution (350 μL, containing 0.2% sodium azide) and 700 μL of melanoidin/AG (positive control)/phosphate buffer (negative control) solutions. The incubation of WP/MGO, WP/GO and WP/glucose model systems was performed for 2, 7 and 14 days at 35 °C. After incubation, samples (0.5 mL) were analyzed for the remaining DCs content in WP/GO and WP/MGO models, as previously described. Acidic hydrolysis followed by hydrophilic interaction liquid chromatography (HILIC) tandem mass spectrometry were performed on the remaining samples to quantify CEL, CML MG-H1 and furosine as described in the next section.

2.8. D-AGEs and furosine quantification by HILIC-tandem mass spectrometry

The determination of CEL, CML, MG-H1 and furosine contents in the samples was performed according to the method of Troise et al. (2015) with modifications. In brief, a 1 mL aliquot of each model system was added to 4 mL of HCl (7.4 M) and then hydrolyzed at 110 °C, for 20 h. After filtering the hydrolysate using a 0.22 μm PVDF filter, 400 μL of each filtrate was dried under vacuum using a rotary evaporator (Eppendorf Concentrator 5310, Hamburg, Germany); 400 μL of 80% aqueous acetonitrile were used to reconstitute the dried samples. To achieve a final concentration of 200 μg/L for each internal standard in each sample, 380 μL of reconstituted sample and 20 μL of the internal standards mix were combined. CEL, CML, MG-H1 and furosine quantitation was achieved by a U-HPLC system (Ultimate 3000 RS, Thermo Fisher Scientific) interfaced to a linear ion trap hybrid Orbitrap high resolution mass spectrometer (LTQ Orbitrap XL, Thermo Fisher Scientific). Chromatographic separation encompassed the use of a sulfobetaine zwitterionic HILIC column (Synchronis HILIC, 100 × 2.1 mm, 1.7 μm, Thermo Fisher Scientific), thermostated at 30 °C, which was eluted with the following gradient of solvent B (minutes/%B): (0/10), (1/10), (6/85), (7/85), with an equilibration stage of 1.5 min. Mobile phases consisted of 0.1% formic acid in acetonitrile (solvent A) and 0.1% formic acid (solvent B), and the flow rate was 0.2 mL/min. LC stream was interfaced to an electrospray ion source (ESI) working in positive ion mode scanning the ion in the m/z range 70–600; resolution was set at 30000 (FWHM at m/z 200), capillary temperature was 320 °C, while sheath and auxiliary gases were set at 30 and 5 arbitrary units, respectively. Analytes profile data in full MS mode were collected using Xcalibur 2.1 (Thermo Fisher Scientific). Calibration curve was performed by internal standard technique in the linearity range 10–10000 ng/mL with four orders of magnitude and a mass accuracy below 3 ppm. Analytical performances are reported in Table A1 in the supplementary material.

2.9. Statistical analysis

Experimental procedures were conducted in three independent replicates. Significant statistical differences ($p < 0.05$) in antioxidant activity, TPC, amino groups content, MGO and GO formation in the glucose model system were analyzed using a one-way ANOVA test. Post hoc analysis was performed via the Tukey's HSD test using the SPSS statistics (v. 26.0, IBM, Armonk, NY). The data distribution normality and the equality of variances were validated using the Shapiro Wilk test and the Levene's test, respectively.

To compare means of MGO/GO trapping ability, CML, CEL, MG-H1/H3 and furosine contents in the WP/DCs and WP/glucose systems, a 2-way repeated measures ANOVA was carried out using the same statistical package. For each dependent variable (MGO trapping capacity, GO trapping capacity, CML, CEL, MG-H1 and furosine contents), incubation time was the within-subjects factor and the treatment (that is LR, IR and HR BSGM in the WP/DCs systems subsequently used for the quantification of amino groups; AG, LR, IR, LR, HR BSGM for the analysis of DCs trapping in the WP/GO and WP/MGO model systems; Control, AG, LR, IR, LR, HR BSGM for the analysis of d-AGEs and furosine) was the between-subjects factor. The interaction between these two factors was also studied. Finally, pairwise comparisons within the same dependent variable in the repeated measures ANOVA models were performed using the Tukey's test. Means were considered significantly different at $p < 0.05$. Normality of data distribution, data sphericity and homogeneity of variances in each treatment were checked using the Shapiro Wilk test, the Mauchly's test and the Levene's test, respectively. As shown in Tables A2–A5 in the supplementary material, for all dependent variables, the data was normally distributed, and variances of data distribution were equal. Assumptions of sphericity for the interaction were also met in all datasets. Finally, the interaction treatment × incubation time was significant for each of the studied dependent variables.

3. Results and discussion

3.1. Antioxidant analyses and TPC of BSGM

Fig. 1 summarizes the functional properties of BSGM in terms of total phenolic contents, antioxidant activity measured through ABTS and FRAP assays, and the ability to chelate MGO and GO. Fig. 1A highlights total phenolic content in the three different roasting processes upon Folin-Ciocalteu's assay; IR and HR BSGM displayed similar concentration of aromatic compounds (161.2 ± 2.5 and 157.4 ± 1.6 mg GAE/100 g dw, respectively) ($p > 0.05$), while LR BSGM (132.4 ± 0.5 mg GAE/100 g dw) had a statistically lower TPC than the other two melanoidins groups among the three types of melanoidins ($p < 0.05$). The TPC measured in this study is lower than those reported in cocoa melanoidins. In fact, in the study conducted by Oracz and Zyzelewicz (2019) investigating cocoa melanoidins from three different varieties and roasted at diverse temperatures and variable levels of relative humidity, it was found that the TPC was in the range of 930.6–1499.0 mg GAE/100 g dw. However, TPC levels measured in BSGM were within the range 50–2750 mg GAE/100 g dw, which is in good agreement with values previously reported by Borrelli et al. (2002) in four different melanoidins fractions of light, medium and dark roasted coffee beans.

Fig. 1B and C report the antioxidant activity of the three types of melanoidins measured by the ABTS and the FRAP assays, respectively. Both analyses corroborated the findings of the TPC assay with IR BSGM showing the highest antioxidant activity (20.2 ± 0.6 mg TEAC/100 g dw and 3.8 ± 0.2 mg GAE/100 g dw for ABTS and FRAP, respectively) ($p < 0.05$). HR BSGM (18.5 ± 0.3 mg TEAC/100 g dw and 3.5 ± 0.1 mg GAE/100 g dw for ABTS and FRAP, respectively) had a higher antioxidant activity ($p < 0.05$) than LR BSGM (16.4 ± 0.1 mg TEAC/100 g dw and 2.9 ± 0.1 mg GAE/100 g dw for ABTS and FRAP, respectively).

The ABTS antioxidant activity of the three types of melanoidins was in line with previous studies on instant coffee melanoidins (Delgado-Andrade et al., 2005; Rufián-Henares and Morales, 2006), with values in the range of 13.3–22.0 mg TEAC/100 g of sample depending on the roasting intensity. Results were also consistent with those outlined by Zhang et al. (2021) that reported an activity ranging from 9.5 to 20.3 mg TEAC/100 g of sample in cocoa melanoidins depending on the roasting degree. These results confirmed the essential role played by roasting parameters in tuning BSGM functional properties ensuing chemical composition modifications and molecular rearrangements in brewer's spent grain, as it was observed in coffee and cocoa (Mesías and Delgado-Andrade, 2017; Quiroz-Reyes and Fogliano, 2018). Besides differences due to the matrices, we hypothesize that the roasting is the main driver for the accumulation of chemical structures with conjugated double bond systems prone to the reaction with the Folin Ciocalteu's reagent.

Table 1 shows that BSGM from the three different roasting regimes trapped both MGO and GO with a final concentration of MGO around 33% lower than GO. MGO and GO trapping significantly increased upon incubation in all tested samples ($p < 0.05$). Within 2 days of incubation,

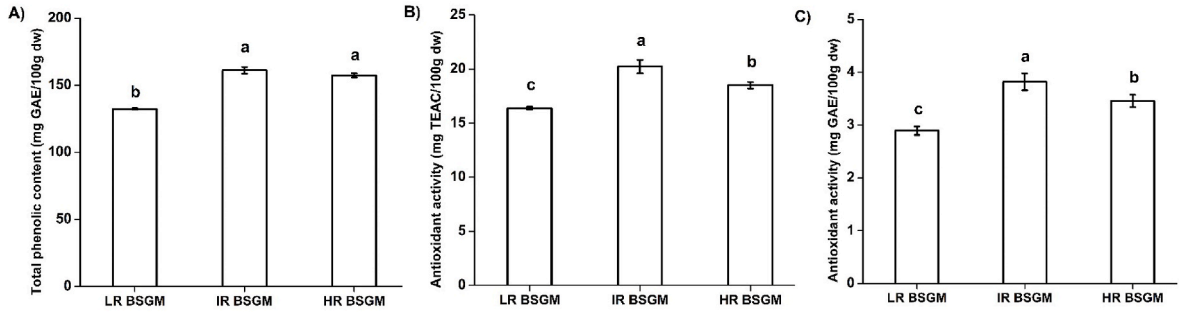

Fig. 1. Total phenolic content (mg gallic acid equivalent/100g dry weight) in low roasted (LR), intermediate roasted (IR) and highly roasted (HR) brewer's spent grain melanoidins (BSGM) (A). Antioxidant activities of LR, IR and HR BSGM following the ABTS (B) and the FRAP (C) assays. Results are expressed in mg Trolox equivalent/100g of dry weight for ABTS and FRAP, respectively. Different letters indicate a significant difference according to Tukey's HSD test at $p < 0.05$. All results are expressed as mean ± SD (n = 3).

Table 1
Time-course study of methylglyoxal (MGO) (1.28 mM) and glyoxal (GO) (1.28 mM) trapping capacity of LR, IR and HR BSGM (10 mg/mL) after 2, 7 and 14 days of incubation. All results are expressed as mean ± SD (n = 3). Low roasted (LR), intermediate roasted (IR) and highly roasted (HR) brewer's spent grain melanoidins (BSGM).

BSGM type	MGO decrease (%)			GO decrease (%)		
	Day 2	Day 7	Day 14	Day 2	Day 7	Day 14
LR BSGM	16.7 ± 1.6 Ab	23.0 ± 2.4 Ba	53.5 ± 2.5 Cb	6.2 ± 2.4 Aab	15.2 ± 2.3 Ba	30.5 ± 1.3 Ca
IR BSGM	18.2 ± 0.8 Ab	34.2 ± 1.1 Bb	61.1 ± 2.5 Cc	10.1 ± 2.4 Ab	21.2 ± 2.4 Bb	42.9 ± 2.2 Cb
HR BSGM	8.9 ± 1.7 Aa	19.7 ± 2.3 Ba	40.8 ± 2.7 Ca	3.6 ± 1.1 Aa	12.9 ± 1.6 Ba	25.6 ± 2.8 Ca

Different uppercase letters in the same raw within a given α-dicarbonyl compound indicate significant differences ($p < 0.05$) according to Tukey's HSD test. Different lowercase letters in the same column within a given α-dicarbonyl compound indicate significant differences ($p < 0.05$) according to Tukey's HSD test.

LR, IR and HR BSGM reduced minimal amounts of MGO, with HR BSGM being the least effective addition ($p < 0.05$), while IR and LR BSGM having a higher and comparable performance. A comparable trend was observed for GO after the same incubation period, with IR BSGM being the most efficient in eliminating GO ($p < 0.05$), followed in order by LR BSGM and HR BSGM.

At 7 days of incubation, IR BSGM exhibited the highest DCs scavenging ability among tested BSGM ($p < 0.05$). At the end of the incubation, IR BSGM maintained the highest trapping rate of both MGO and GO amongst the tested BSGM types ($p < 0.05$). No significant difference was observed in LR and HR BSGM trapping rates of GO ($p > 0.05$). LR BSGM trapped more MGO than HR BSGM ($p < 0.05$). The specific affinity of MGO for hydroxyalkylation and aromatic substitution was in line with results from previous studies (Nigro et al., 2019; Blidi et al., 2023), suggesting that no steric hindrance is being exerted by the methyl group of MGO (Zhang et al., 2021). Our quantitative results differed from those of Zhang et al. (2021) that reported GO decreases ranging between 45.3 and 67.8% and MGO reductions from approximately 75 to 90% within the same incubation time. This might be due to the difference in roasting conditions and to the higher polyphenols content in cocoa melanoidins compared to BSGM. Furthermore, we cannot exclude the intrinsic reactivity of polyphenols in combination with the local accumulation of C-7 and C-5 dihydroxy-substituted A ring undergoing carbonyl substitutions on C-6 and C-8 (Lund, 2021). Indeed, the higher TPC and antioxidant activity in IR BSGM could be the reason behind its higher trapping activity when compared to that of LR and HR BSGM. This is supported by existing data on cocoa melanoidins, where the intermediate roasting conditions resulted in the highest TPC and antioxidant activity in the studied samples (Oracz and Zyzelewicz, 2019; Oracz et al., 2019). Furthermore, the spatial orientation of the melanoidin-bound phenolic groups, affected by the roasting intensity, might also contribute to the difference in the trapping ability of the tested BSGM groups.

Table 2 outlines the amino groups content in the melanoidins samples. Prior findings established that the melanoidin-bound polyphenols fraction is primarily responsible for food melanoidins DCs trapping ability (H. Zhang et al., 2019). This time-course study focused on the contribution of amino groups present in melanoidins in scavenging DCs. In the control samples, a decrease in amino groups content was observed with the increase of roasting intensity. This could be due to the involvement of the free amino groups present in the melanoidin-bound proteins in chemical reactions with sugars, polyphenols, and other components, leading to different structural arrangement of melanoidins. These reactions are promoted by the severe roasting conditions (Wang et al., 2011).

Amino groups content diminished in the presence of DCs with increasing incubation time. A faster reduction was observed in the presence of MGO than GO ($p < 0.05$), which indicates the significant reactivity of MGO toward amino groups (Prestes et al., 2017). This result was in agreement with the findings of Zhang et al. (2021), which reported decreases of available amino groups in cocoa melanoidins in the ranges of 21.4–39.6% and 3.0–9.6%, in the presence of MGO and GO, respectively, depending on the roasting intensity and the incubation

Table 2
Amino groups content (μmol/g of melanoidins) in low roasted (LR), intermediate roasted (IR) and highly roasted (HR) brewer's spent grain melanoidins (BSGM) after 2, 7 and 14 days of incubation with or without glyoxal (GO) and methylglyoxal (MGO). Data are presented as the mean ± SD (n = 3).

	Control	GO	MGO
LR BSGM			
0 days	79.1 ± 3.2 a		
2 days	78.7 ± 1.4 a	77.1 ± 1.3 a	66.0 ± 1.8 de
7 days	78.8 ± 0.7 a	72.4 ± 2.2 BCE	62.5 ± 1.1 ef
14 days	76.9 ± 0.7 ab	70.2 ± 0.8 cd	58.5 ± 0.7 f
IR BSGM			
0 days	71.0 ± 1.2 a		
2 days	69.8 ± 0.8 a	61.7 ± 1.7 b	60.3 ± 1.0 b
7 days	70.6 ± 0.5 a	63.1 ± 1.6 b	59.1 ± 1.1 BCE
14 days	69.4 ± 1.0 a	55.0 ± 2.8 c	49.0 ± 2.1 d
HR BSGM			
0 days	63.7 ± 1.3 a		
2 days	63.5 ± 2.1 a	62.0 ± 1.2 ab	61.2 ± 1.3 ab
7 days	59.2 ± 0.4 b	54.4 ± 0.6 de	51.2 ± 0.9 e
14 days	56.5 ± 0.7 c	51.3 ± 1.0 e	46.1 ± 1.2 f

Different letters in the same melanoidins group express a significant statistical difference following the Tukey's HSD test at $p < 0.05$.

duration. After 14 days of incubation, the most important decrease was observed in IR BSGM samples in both systems ($p < 0.05$). This finding was in line with the DCs scavenging data discussed hereabove. Based on the composition of the studied model system, the amount of amino groups in the different BSGM types was in the range of 0.14–0.20 μmol, which is 7.7–11 times lower than DCs content (1.54 μmol), showing the prevailing contribution of melanoidin-bound polyphenols in trapping DCs.

3.2. Effect of BSGM on the formation of CML in the WP/GO model system

The capacity of BSGM to inhibit the formation of CML was measured in the WP/GO reaction model system. CML is one of the most studied glycation compounds due to the possibility that its formation can occur in both food systems and *in vivo*. From a chemical point of view, CML is one of the best characterized AGEs and can be considered as a MR marker in food systems (Delgado-Andrade, 2016). Moreover, dairy-based products contain a significant CML content in comparison to other foods (Assar et al., 2009). Fig. 2A reveals that GO trapping capacity of the three melanoidin-containing systems increased during incubation. Considering the BSGM groups, GO levels were most effectively reduced in the presence of IR BSGM throughout the incubation span ($p < 0.05$) with a decrease of 50.9 ± 3.0%, after 14 days of incubation. In accordance with the results on trapping activity without WP (Table 1), in presence of proteins, LR BSGM reduced more GO than HR BSGM at 2 days of incubation ($p < 0.05$), although these trapping rates did not exceed 9%. No statistically significant difference between these two groups was observed at later incubation times ($p > 0.05$), with both extracts trapping approximately 15 and 40% of GO at days 7 and 14, respectively. As a positive control, AG showed a high affinity towards GO from the early incubation stages, trapping 86.4 ± 0.2% of GO within two days. AG was the most effective compound in scavenging GO among all tested samples ($p < 0.05$) throughout the whole incubation period.

Fig. 2B shows the CML generated during the 14-day incubation of the WP/GO model system. When compared to day 2, significant CML amounts were formed starting from day 7 until day 14 in the control reaction model system ($p < 0.05$). Regarding melanoidin groups, CML concentration was most effectively mitigated in the presence of IR BSGM at days 7 and 14 ($p < 0.05$), with decreases of 18.8 and 25.4%, respectively, compared to the control sample. LR and HR BSGM samples displayed similar CML content ($p > 0.05$) on day 7. On day 14, the HR BSGM group showed statistically lower CML content than LR BSGM samples ($p < 0.05$). These findings can be explained by the evidence that higher amounts of GO were trapped by IR BSGM than by HR and LR BSGM. This supported the hypothesis that BSGM can mitigate the formation of CML in WP system via direct GO scavenging. In the presence of AG, CML concentration was lowered by more than 95% after 14 days of incubation. This was associated with the high GO scavenging showcased by AG. All numerical data of the WP/GO system can be found in Table A6 in the supplementary material.

3.3. Effect of BSGM on CEL and MG-H1/H3 formation in the WP/MGO model system

In a similar way to the WP/GO model system, in Fig. 3 we described the key role of MGO in generating two glycation end products, respectively formed on guanidino side chain of arginine (MG-H1) and epsilon amino group of lysine (CEL). Acid hydrolysis conditions lead to isomeric conversion of MG-H1 to methylglyoxal-hydroimidazolone 3 (MG-H3) (Akıllıoğlu and Lund, 2022); therefore MG-H1 was represented by the sum of the two isomers (MG-H1/H3). The MGO trapping capacity of BSGM in the WP/MGO model system is summarized in Fig. 3A. In the melanoidin groups, after 7 days, IR BSGM was again more effective in trapping MGO than HR BSGM ($p < 0.05$), which was in turn more effective than LR BSGM ($p < 0.05$). This result was extended throughout the incubation; at 14 days, IR BSGM blocked more MGO than the other melanoidin types ($p < 0.05$). with more than half of the available MGO trapped, followed in order by LR BSGM and HR BSGM ($p < 0.05$). On the other hand, AG quenched more than 90% of MGO within 2 days of incubation, showing a higher DCs inhibition potency than melanoidins until the end of the incubation span ($p < 0.05$).

The concentration of CEL was 186.6 ± 6.1 μM in the control sample after 14 days of incubation (Fig. 3B). In the presence of IR and HR BSGM, the concentration of CEL was slightly higher than that in the control sample ($p < 0.05$), with final relative increases of 11.9 and 16.7%, respectively. AG was an effective inhibitor of CEL showing only 0.7 ± 0.2, 15.4 ± 2.0 and 17.6 ± 1.8 μM of CEL after 2, 7 and 14 days of incubation.

Fig. 3C shows the effect of BSGM on the formation of MG-H1/H3. After 14 days of incubation, the control sample had a content of MG-H1/H3 higher than that of CEL. This finding was in line with the values reported by W. Zhang et al. (2019) showing MG-H1 as the most prominent d-AGE deriving from MGO in lactose-hydrolyzed milk during storage. The role of arginine modifications has received less attention than lysine modifications; however, in terms of total exposure to advanced glycation products, concentration of hydroimidazolones often exceed those of lysine modifications such as CML, CEL and pyrraline (Scheijen et al., 2016). In particular, looking at dairy products as infant formulas and their substitute with vegetable proteins, MG-H1 becomes a relevant concern as recently outlined by Xie et al. (2023).

Furthermore, it was observed that BSGM were relatively better

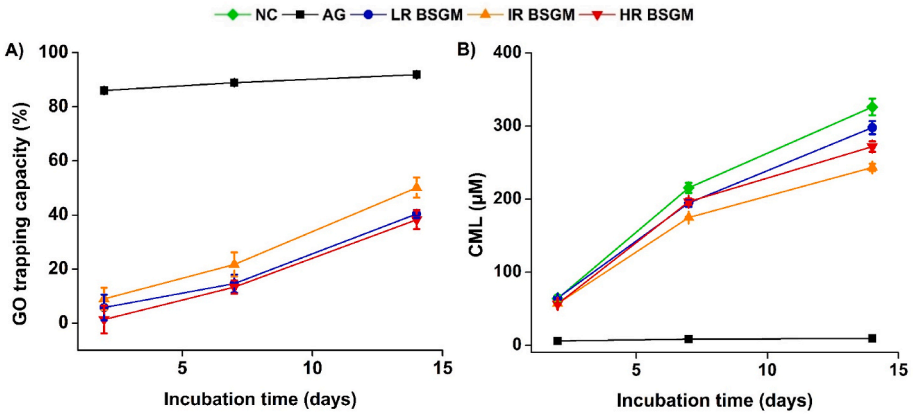

Fig. 2. Glyoxal (GO) trapping capacity (A) and *N*-ε-carboxymethyllysine (CML) (B) content in the presence of the three brewer's spent grains melanoidins (10 mg/mL) and aminoguanidine (AG) (4 mg/mL) in the whey protein/GO model system after 2, 7 and 14 days of incubation at 35 °C. Results are expressed as mean ± SD (n = 3). Low roasted (LR), intermediate roasted (IR) and highly roasted (HR) brewer's spent grain melanoidins (BSGM); negative control (NC).

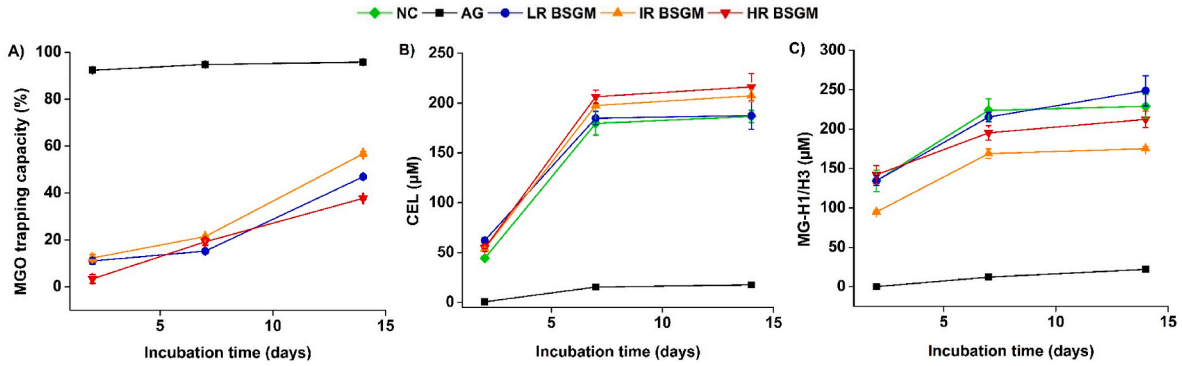

Fig. 3. Methylglyoxal (MGO) trapping capacity (A), *N*-ε-carboxyethyllysine (CEL) (B) and methylglyoxal-derived hydroimidazolone 1/3 (MG-H1/H3) (C) contents in the presence of the three brewer's spent grain melanoidins (10 mg/mL) and aminoguanidine (AG) (4 mg/mL) in the whey protein/MGO model system after 2, 7 and 14 days of incubation at 35 °C. Results are expressed as mean ± SD (n = 3). Low roasted (LR), intermediate roasted (IR) and highly roasted (HR) brewer's spent grain melanoidins (BSGM); negative control (NC).

inhibitors of MG-H1/H3 than of CEL, especially in the case of IR BSGM that significantly reduced MG-H1/H3 content by 29.4, 24.6 and 23.5% compared to the control sample, after 2, 7 and 14 days of incubation, respectively ($p < 0.05$). Generally, HR BSGM did not greatly reduce MG-H1/H3 content ($p > 0.05$), mitigating only 7.3% of MG-H1/H3 content relative to the control after the entirety of the incubation period. Furthermore, no MG-H1/H3 reduction ($p > 0.05$) was observed in the presence of LR BSGM on days 2 and 7. After the whole incubation time span, the presence of LR BSGM slightly promoted the formation of MG-H1/H3 in analogy to the control. However, this increase was not statistically significant ($p > 0.05$). Finally, AG was the most effective MG-H1/H3 inhibitor ($p < 0.05$), with no MG-H1/H3 found after 2 days of incubation and only 22.0 ± 2.2 μM at the end of the incubation period. All numerical data of the WP/MGO system are reported in Table A7 in the supplementary material.

Considering the results from all the model systems, BSGM were less active in reducing the concentration of MGO-derived lysine AGEs as CEL than of GO-derived AGEs as CML. A possible explanation to this finding lies in the fact that the remaining MGO is more reactive than the remaining GO toward amino acids in WP. Such results are in line with what previously described for multi-response modelling of CML and CEL formation (Nguyen et al., 2016). However, the role of DCs offers only a partial explanation to the overall formation of lysine glycation products and the overall mechanistic insight needs to include other fragmentation

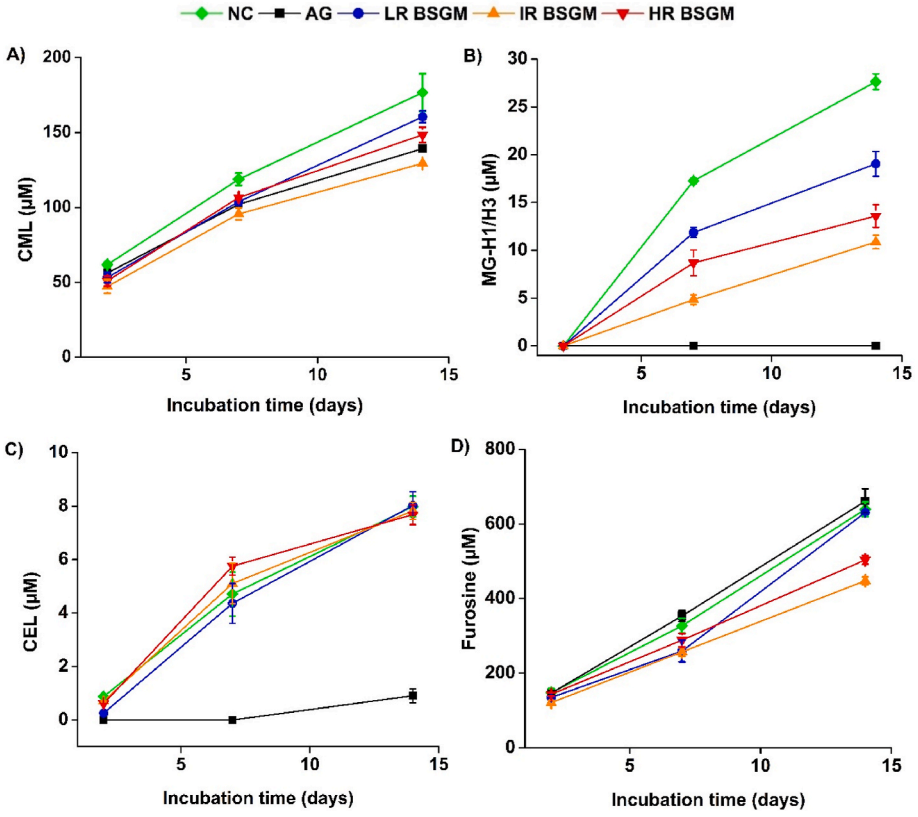

Fig. 4. Effect of three brewer's spent grains melanoidins (10 mg/mL) and aminoguanidine (AG) (4 mg/mL) on the formation of *N*-ε-carboxymethyllysine (CML) (A), methylglyoxal-derived hydroimidazolone 1 and 3 (MG-H1/H3) (B), *N*-ε-carboxyethyllysine (CEL) (C) and furosine (D) in the whey protein/glucose model system after 2, 7 and 14 days of incubation at 35 °C. Results are expressed as mean ± SD (n = 3). Low roasted (LR), intermediate roasted (IR) and highly roasted (HR) brewer's spent grain melanoidins (BSGM); negative control (NC).

products arising from glucose degradation (Kasper and Schieberle, 2005). In the case of arginine modifications, no clear conclusion can be drawn regarding the preferential reduction of arginine-GO adduct or arginine-MGO formation as no arginine-GO adduct was detected in the control model systems. Therefore, it is fundamental to consider DCs reactivity with proteins when associating DCs trapping capacity to the mitigation of protein glycation.

3.4. Effect of BSGM on d-AGEs and furosine formation in the WP/glucose model system

To investigate the inhibitory effects of BSGM against WP glycation, glucose was used as a substrate given its higher reactivity towards amino groups, compared to lactose (Troise et al., 2016). Full numerical data of the WP/MGO system are reported in Tables A8–A11 in the supplementary material. As shown in Fig. 4A, all three BSGM types significantly hindered the formation of CML in the WP/glucose model system, with IR BSGM being the most effective group ($p < 0.05$), suppressing 19.5 and 26.7% of CML compared to the control after 7 and 14 days of incubation, respectively. This finding could be linked to the higher GO scavenging of IR BSGM compared to the other two BSGM types tested. AG did not inhibit the formation of CML as efficiently as in the WP/GO model system, with a maximum reduction of 21.1% after 14 days of incubation, compared to the control.

Regarding arginine modifications, no MG-H1/H3 was detected in any of the samples after 2 days of incubation (Fig. 4B). This can be related to a slower MGO formation in the glucose model system than in the model system with added MGO. The control sample displayed the highest MG-H1/H3 contents in the subsequent time points ($p < 0.05$) with respective values of 17.3 ± 0.3 and 27.6 ± 1.1 μM. All three BSGM types limited the development of MG-H1/H3 in the WP/glucose reaction system ($p < 0.05$). After 14 days and in the presence of IR BSGM, only 39.5% of MG-H1/H3 of the control sample remained. AG was the most effective compound in inhibiting MG-H1/H3, with concentrations below the detection limit after 14 days. These findings are in line with the MGO trapping capacities of the different types of BSGM reported in the WP/MGO model system.

Furthermore, only the AG group was efficient in limiting the formation of CEL ($p < 0.05$), with only 0.9 ± 0.3 μM of CEL present after the maximal incubation time elapsed (Fig. 4C). Contrarily, in the presence of BSGM, CEL concentrations matched that of the control ($p > 0.05$), suggesting no involvement of melanoidins in the inhibition of CEL formation. Nevertheless, the concentration of CEL in the WP/glucose was significantly lower than those of MG-H1/H3 and CML, indicating that the MGO formed following glucose degradation preferentially undergoes reaction with arginine rather than lysine (Schalkwijk, 2015). However, along with the most prominent MGO-mediated oxidation pathway, we hypothesize that CEL can be putatively formed also from preliminary isomerization of glucose into fructose and subsequent fragmentation of the Heyns product glucosyllysine, as reported by Şen and Gökmen (2022) in roasted nuts and seeds. The role of BSGM can be relevant but longer incubation times are required for the WP/glucose model system to allow a more significant CEL formation.

The effect of BSGM in the formation of Amadori products that are formed during the initial stages of MR was also investigated through the quantification of furosine. Fig. 4D shows that only IR and HR BSGM significantly reduced the development of furosine in the WP/glucose model system ($p < 0.05$) with decreases of 30.0 and 21.2% after 14 days of incubation, respectively. On other hand, in the AG group, the concentration of furosine was similar that of the control group, indicating no effect of AG on the formation of furosine during the incubation ($p > 0.05$). AG, through its guanidino groups, seemed less prone to react with amino groups of WP and most of its inhibition activity toward d-AGEs might come from its DCs scavenging activity.

All together, these outcomes revealed the ability of BSGM in controlling protein-bound lysine glycation through numerous routes. In Fig. 5, we summarize the putative key mechanisms behind the role of melanoidins in reducing both DCs and d-AGEs. Under roasting conditions, melanoidin-bound phenolic rings can be oxidized to quinones, which are highly reactive with amino groups present in WP, thus

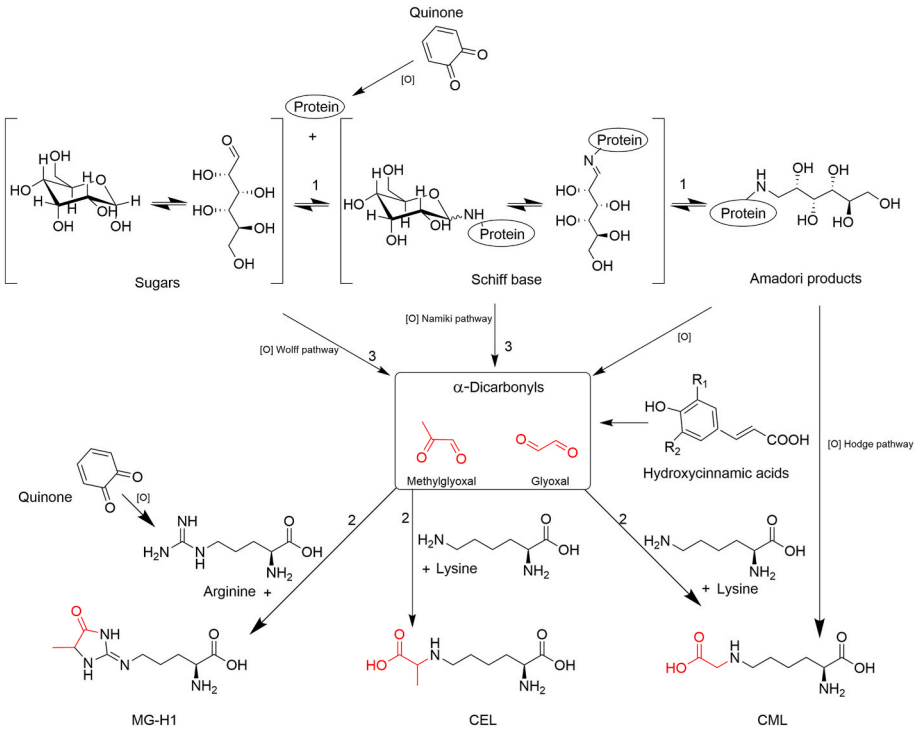

Fig. 5. Proposed mechanisms for the inhibition of *N*-ε-carboxymethyllysine (CML) and methylglyoxal-derived hydroimidazolone 1 (MG-H1) by high-molecular-weight brewer's spent grain melanoidins through decrease of protein-bound Amadori products (Route 1), α-dicarbonyl compounds scavenging (Route 2) or blockage of oxidative fragmentation of Schiff bases and sugars (Route 3).

limiting the ability of glucose and its degradation products to access reaction sites available in proteins (Guerra and Yaylayan, 2014). The interaction between WP and glucose can be partially disrupted by the presence of the macromolecule derived from melanoidins and WP through steric hindrance.

The trend observed in the different lysine Amadori compounds measured through furosine concentrations in the WP/glucose model system could be behind the fact that BSGM were more active than AG in limiting the formation of CML in the WP/glucose model system but less efficient in the WP/GO model system. Similar findings have been reported by Zhang et al. (2021), who observed that cocoa melanoidins reduced CML more effectively than AG in WP/glucose, while the contrary was noticed in the WP/GO model system.

The concurrent reduction of furosine and CML in the WP/glucose model system in the presence of BSGM highlights the fact that these compounds are also effective in mitigating the formation of CML by limiting lysine Amadori compound generation (Fig. 5, route 1). On the other hand, AG was unable to suppress any furosine in the WP/glucose model system despite reducing 21.2, 90.7 and 100% of CML, CEL and MG-H1/H3, respectively, after 14 days of incubation. This implies that AG is effective in limiting d-AGEs formation mainly through scavenging DCs generated during MR (Fig. 5, route 2) (Glomb and Monnier, 1995). This was further confirmed by the results obtained from the WP/DCs model systems.

Glycation compounds can also be generated through the Namiki and Wolff pathways involving the nucleophilic attack of amino, guanidino and thiol groups of proteins and peptides on free DCs generated from the fragmentation of sugars and Schiff bases (Fig. 5, route 3) (Namiki and Hayashi, 1983; Wolff and Dean, 1987). The significant simultaneous decrease of MGO and GO contents as well as the concentrations of their respective d-AGEs by AG and BSGM suggests the Namiki pathway had a pertinent role in the formation of d-AGEs in WP/glucose model system and that AG was more effective than BSGM in blocking this pathway by scavenging more DCs formed by degradation of Schiff bases as shown in the WP/glucose model system. The effect of melanoidins on the Wolff pathway resulting from the oxidation of free sugars was further investigated by assessing MGO and GO formation during the incubation of glucose in the presence or absence of BSGM/AG. Fig. A1 in the supplementary material indicates that the control group developed more GO than MGO with prolonged incubation times, reaching 77.6 ± 1.1 and 12.2 ± 0.5 μM after 14 days of incubation, respectively.

In the presence of IR BSGM, MGO concentrations significantly decreased ($p < 0.05$) compared to the control amounting to 0.9 ± 0.0 μM after 14 days of incubation. The same trend was observed for GO with a concentration declining to 5.2 ± 0.3 μM after the same incubation time. Moreover, AG reduced the studied DCs more effectively than IR BSGM ($p < 0.05$), with no MGO and GO detected at the end of the incubation time. This supports the findings that AG was more effective than BSGM in inhibiting DCs generation from the auto oxidation of sugar through the Wolff pathway.

In addition to the direct GO and MGO scavenging, transition metals sequestration is a potent way to mitigate DCs formation from glucose as demonstrated in previous studies (Chetyrkin et al., 2011). Therefore, the capacity of BSGM in blocking oxidative stress through their antioxidant properties and their metal ion-chelating activity can be another effective route able to keep under control the transition metal coordination reaction of reducing sugars and amino groups of proteins (Morales et al., 2012). These can be two key components in controlling the Wolff pathway and, by extension, the Namiki pathway, as both mechanisms necessitate the presence of transition metals such as copper and iron as well as glucose. This could also explain the higher antiglycative activity of IR BSGM in comparison to that of LR and HR BSGM.

4. Conclusion

This study demonstrates the ability of BSGM in inhibiting the formation of CML and MG-H1/H3 in WP model systems during incubation at 35 °C for up to 14 days. Their trapping effectiveness was conditioned by the roasting parameters of BSG and to the consequent formation of reactive sites in combination with better bioavailability of polyphenols through spatial orientation. A key role was represented by glucose and its capacity in generating highly reactive carbonyl structures potentially involved in the formation of advanced glycation products. By monitoring the concentration of furosine and investigating glucose degradation, we demonstrated that BSGM could limit the extent of MR mainly via three different mechanisms: *i*) inhibiting Amadori products generation; *ii*) direct trapping of DCs, like MGO and GO, resulting from MR intermediates and glucose fragmentation; *iii*) hindering of glucose and MR intermediates oxidation. Melanoidin-bound polyphenols can be considered as a valuable pool of bioactive compounds, whose affinity towards reactive species can be improved via thermal treatment such as roasting. Based on different reaction pathways, it was demonstrated that the use of BSGM represents a challenging approach to mitigate the formation of d-AGEs in dairy products under extreme storage conditions to potentially promote the safety and quality of flavored milk beverages.

CRediT authorship contribution statement

Slim Blidi: Conceptualization, Methodology, Investigation, Data curation, Formal analysis, Validation, Writing – original draft, Visualization. **Antonio Dario Troise:** Investigation, Formal analysis, Writing – original draft, Writing – review & editing, Visualization, Resources. **Mattia Zazzaroni:** Investigation, Formal analysis, Writing – review & editing. **Sabrina De Pascale:** Investigation, Formal analysis, Data curation, Resources. **Sarah Cottin:** Conceptualization, Supervision, Writing – review & editing. **Keith Sturrock:** Conceptualization, Supervision, Funding acquisition, Writing – review & editing. **Andrea Scaloni:** Resources, Writing – review & editing, Project administration. **Alberto Fiore:** Conceptualization, Supervision, Funding acquisition, Writing – review & editing, Project administration.

Declaration of competing interest

The authors declare that they have no known competing financial interests or personal relationships that could have appeared to influence the work reported in this paper.

Data availability

Data will be made available on request.

Acknowledgements

We gratefully acknowledge the financial support from the Abertay University R-LINCS studentship allowing the conduct of the research and the preparation of the article. This work was also supported by grants from: the Italian National Research Council for the project “Nutrizione, Alimentazione ed Invecchiamento Attivo (NUTRAGE)” (FOE-2021-2022); the National Recovery and Resilience Plan, mission 4, component 2, investment 1.3, MUR call n. 341/2022 funded by the European Union-NextGenerationEU for the project “ON-FOODS - Research and innovation network on food and nutrition Sustainability, Safety and Security-Working ON Foods”, concession decree n. 1550/2022, PE00000003, CUP B83C22004790001. This manuscript reflects only the authors’ views and opinions, neither the European Union nor the European Commission can be considered responsible for them.

Appendix A. Supplementary data

Supplementary data to this article can be found online at https://doi.org/10.1016/j.crfs.2024.100767.

References

Akıllıoğlu, H.G., Lund, M.N., 2022. Quantification of advanced glycation end products and amino acid cross-links in foods by high-resolution mass spectrometry: applicability of acid hydrolysis. Food Chem. 366, 130601 https://doi.org/10.1016/j.foodchem.2021.130601.

Assar, S.H., Moloney, C., Lima, M., Magee, R., Ames, J.M., 2009. Determination of N ε-(carboxymethyl)lysine in food systems by ultra performance liquid chromatography-mass spectrometry. Amino Acids 36, 317–326. https://doi.org/10.1007/s00726-008-0071-4.

Benzie, I.F.F., Strain, J.J., 1996. The ferric reducing ability of plasma (FRAP) as a measure of "antioxidant power": the FRAP assay. Anal. Biochem. 239, 70–76. https://doi.org/10.1006/abio.1996.0292.

Blidi, S., Troise, A.D., Ledbetter, M., Cottin, S., Sturrock, K., De Pascale, S., Scaloni, A., Fiore, A., 2023. α-Dicarbonyl compounds trapping ability and antiglycative effect of high-molecular-weight brewer's spent grain melanoidins. LWT 180, 114679. https://doi.org/10.1016/j.lwt.2023.114679.

Bork, L.V., Stobernack, T., Rohn, S., Kanzler, C., 2024. Browning reactions of hydroxycinnamic acids and heterocyclic Maillard reaction intermediates – formation of phenol-containing colorants. Food Chem. 449, 139189 https://doi.org/10.1016/j.foodchem.2024.139189.

Borrelli, R.C., Visconti, A., Mennella, C., Anese, M., Fogliano, V., 2002. Chemical characterization and antioxidant properties of coffee melanoidins. J. Agric. Food Chem. 50, 6527–6533. https://doi.org/10.1021/jf025686o.

Chetyrkin, S., Mathis, M., Pedchenko, V., Sanchez, O.A., McDonald, W.H., Hachey, D.L., Madu, H., Stec, D., Hudson, B., Voziyan, P., 2011. Glucose autoxidation induces functional damage to proteins via modification of critical arginine residues. Biochemistry 50, 6102–6112. https://doi.org/10.1021/bi200757d.

Delgado-Andrade, C., 2016. Carboxymethyl-lysine: thirty years of investigation in the field of AGE formation. Food Funct. 7, 46–57. https://doi.org/10.1039/C5FO00918A.

Delgado-Andrade, C., Fogliano, V., 2018. Dietary advanced glycosylation end-products (dAGEs) and melanoidins formed through the maillard reaction: physiological consequences of their intake. Annu. Rev. Food Sci. Technol. 9, 271–291. https://doi.org/10.1146/annurev-food-030117-012441.

Delgado-Andrade, C., Rufián-Henares, J.A., Morales, F.J., 2005. Assessing the antioxidant activity of melanoidins from coffee brews by different antioxidant methods. J. Agric. Food Chem. 53, 7832–7836. https://doi.org/10.1021/jf0512353.

Glomb, M.A., Monnier, V.M., 1995. Mechanism of protein modification by glyoxal and glycolaldehyde, reactive intermediates of the Maillard reaction. J. Biol. Chem. 270, 10017–10026. https://doi.org/10.1074/jbc.270.17.10017.

Guerra, P.V., Yaylayan, V.A., 2014. Interaction of flavanols with amino acids: postoxidative reactivity of the B-ring of catechin with Glycine. J. Agric. Food Chem. 62, 3831–3836. https://doi.org/10.1021/jf5005989.

Hellwig, M., Henle, T., 2014. Baking, ageing, diabetes: a short history of the maillard reaction. Angew. Chem. Int. Ed. 53, 10316–10329. https://doi.org/10.1002/anie.201308808.

Jenness, R., 1979. The composition of human milk. Semin. Perinatol. 3, 225–239.

Karlsson, M.A., Langton, M., Innings, F., Malmgren, B., Höjer, A., Wikström, M., Lundh, Å., 2019. Changes in stability and shelf-life of ultra-high temperature treated milk during long term storage at different temperatures. Heliyon 5 (9), eo2431. https://doi.org/10.1016/j.heliyon.2019.e02431.

Kasper, M., Schieberle, P., 2005. Labeling studies on the formation pathway of N $^{\varepsilon}$ -carboxymethyllysine in maillard-type reactions. Ann. N. Y. Acad. Sci. 1043, 59–62. https://doi.org/10.1196/annals.1333.007.

Ledbetter, M., Blidi, S., Ackon, S., Bruno, F., Sturrock, K., Pellegrini, N., Fiore, A., 2021. Effect of novel sequential soaking treatments on Maillard reaction products in potato and alternative vegetable crisps. Heliyon 7 (7), eo7441. https://doi.org/10.1016/j.heliyon.2021.e07441.

Lund, M.N., 2021. Reactions of plant polyphenols in foods: impact of molecular structure. Trends Food Sci. Technol. 112, 241–251. https://doi.org/10.1016/j.tifs.2021.03.056.

Lund, M.N., Ray, C.A., 2017. Control of maillard reactions in foods: strategies and chemical mechanisms. J. Agric. Food Chem. 65, 4537–4552. https://doi.org/10.1021/acs.jafc.7b00882.

Mehta, B.M., Deeth, H.C., 2016. Blocked lysine in dairy products: formation, occurrence, analysis, and nutritional implications. Rev. Food Sci. Food Saf. 15, 206–218. https://doi.org/10.1111/1541-4337.12178.

Mesías, M., Delgado-Andrade, C., 2017. Melanoidins as a potential functional food ingredient. Curr. Opin. Food Sci. 14, 37–42. https://doi.org/10.1016/j.cofs.2017.01.007.

Morales, F.J., Somoza, V., Fogliano, V., 2012. Physiological relevance of dietary melanoidins. Amino Acids 42, 1097–1109. https://doi.org/10.1007/s00726-010-0774-1.

Namiki, M., Hayashi, T., 1983. A new mechanism of the maillard reaction involving sugar fragmentation and free radical formation. In: Waller, G.R., Feather, M.S. (Eds.), The Maillard Reaction in Foods and Nutrition, ACS Symposium Series. American Chemical Society, Washington, D.C., pp. 21–47. https://doi.org/10.1021/bk-1983-0215

Nguyen, H.T., Van Der Fels-Klerx, H.J., Van Boekel, M.A.J.S., 2016. Kinetics of Nε-(carboxymethyl)lysine formation in aqueous model systems of sugars and casein. Food Chem. 192, 125–133. https://doi.org/10.1016/j.foodchem.2015.06.110.

Nielsen, P.M., Petersen, D., Dambmann, C., 2001. Improved method for determining food protein degree of hydrolysis. J. Food Sci. 66, 642–646. https://doi.org/10.1111/j.1365-2621.2001.tb04614.x.

Nigro, C., Leone, A., Fiory, F., Prevenzano, I., Nicolò, A., Mirra, P., Beguinot, F., Miele, C., 2019. Dicarbonyl stress at the crossroads of healthy and unhealthy aging. Cells 8, 749. https://doi.org/10.3390/cells8070749.

Oracz, J., Nebesny, E., Żyżelewicz, D., 2019. Identification and quantification of free and bound phenolic compounds contained in the high-molecular weight melanoidin fractions derived from two different types of cocoa beans by UHPLC-DAD-ESI-HR-MSn. Food Res. Int. 115, 135–149. https://doi.org/10.1016/j.foodres.2018.08.028.

Oracz, J., Zyzelewicz, D., 2019. In vitro antioxidant activity and FTIR characterization of high-molecular weight melanoidin fractions from different types of cocoa beans. Antioxidants 8, 560. https://doi.org/10.3390/antiox8110560.

Pischetsrieder, M., Henle, T., 2012. Glycation products in infant formulas: chemical, analytical and physiological aspects. Amino Acids 42, 1111–1118. https://doi.org/10.1007/s00726-010-0775-0.

Prestel, S., de Falco, B., Blidi, S., Fiore, A., Sturrock, K., 2020. Evaluation of the effect of berry extracts on carboxymethyllysine and lysine in ultra-high temperature treated milk. Food Res. Int. 130, 108923 https://doi.org/10.1016/j.foodres.2019.108923.

Prestes, A. de S., dos Santos, M.M., Ecker, A., Zanini, D., Schetinger, M.R.C., Rosemberg, D.B., da Rocha, J.B.T., Barbosa, N.V., 2017. Evaluation of methylglyoxal toxicity in human erythrocytes, leukocytes and platelets. Toxicol. Mech. Methods 27, 307–317. https://doi.org/10.1080/15376516.2017.1285971.

Quiroz-Reyes, C.N., Fogliano, V., 2018. Design cocoa processing towards healthy cocoa products: the role of phenolics and melanoidins. J. Funct.Foods 45, 480–490. https://doi.org/10.1016/j.jff.2018.04.031.

Román, S., Sánchez-Siles, L.M., Siegrist, M., 2017. The importance of food naturalness for consumers: results of a systematic review. Trends Food Sci. Technol. 67, 44–57. https://doi.org/10.1016/j.tifs.2017.06.010.

Roy, B.D., 2008. Milk: the new sports drink? A Review. J. Int. Soc. Sports Nutr. 5, 15. https://doi.org/10.1186/1550-2783-5-15.

Rufián-Henares, J.A., Morales, F.J., 2006. A new application of a commercial microtiter plate-based assay for assessing the antimicrobial activity of Maillard reaction products. Food Res. Int. 39, 33–39. https://doi.org/10.1016/j.foodres.2005.06.002.

Schalkwijk, C.G., 2015. Vascular AGE-ing by methylglyoxal: the past, the present and the future. Diabetologia 58, 1715–1719. https://doi.org/10.1007/s00125-015-3597-5.

Scheijen, J.L.J.M., Clevers, E., Engelen, L., Dagnelie, P.C., Brouns, F., Stehouwer, C.D.A., Schalkwijk, C.G., 2016. Analysis of advanced glycation endproducts in selected food items by ultra-performance liquid chromatography tandem mass spectrometry: presentation of a dietary AGE database. Food Chem. 190, 1145–1150. https://doi.org/10.1016/j.foodchem.2015.06.049.

Şen, D., Gökmen, V., 2022. Kinetic modeling of Maillard and caramelization reactions in sucrose-rich and low moisture foods applied for roasted nuts and seeds. Food Chem. 395, 133583 https://doi.org/10.1016/j.foodchem.2022.133583.

Troise, A.D., Buonanno, M., Fiore, A., Monti, S.M., Fogliano, V., 2016. Evolution of protein bound Maillard reaction end-products and free Amadori compounds in low lactose milk in presence of fructosamine oxidase I. Food Chem. 212, 722–729. https://doi.org/10.1016/j.foodchem.2016.06.037.

Troise, A.D., Fiore, A., Wiltafsky, M., Fogliano, V., 2015. Quantification of Nε-(2-Furoylmethyl)-l-lysine (furosine), Nε-(Carboxymethyl)-l-lysine (CML), Nε-(Carboxyethyl)-l-lysine (CEL) and total lysine through stable isotope dilution assay and tandem mass spectrometry. Food Chem. 188, 357–364.

van Boekel, M., Fogliano, V., Pellegrini, N., Stanton, C., Scholz, G., Lalljie, S., Somoza, V., Knorr, D., Jasti, P.R., Eisenbrand, G., 2010. A review on the beneficial aspects of food processing. Mol. Nutr. Food Res. 54, 1215–1247. https://doi.org/10.1002/mnfr.200900608.

Walker, J.M., Mennella, I., Ferracane, R., Tagliamonte, S., Holik, A.-K., Hölz, K., Somoza, M.M., Somoza, V., Fogliano, V., Vitaglione, P., 2020. Melanoidins from coffee and bread differently influence energy intake: a randomized controlled trial of food intake and gut-brain axis response. J. Funct.Foods 72, 104063. https://doi.org/10.1016/j.jff.2020.104063.

Walstra, P., Wouters, J.T.M., Geurts, T.J., 2005. Dairy Science and Technology, 2 ed. CRC Press. https://doi.org/10.1201/9781420028010.

Wang, H.-Y., Qian, H., Yao, W.-R., 2011. Melanoidins produced by the Maillard reaction: structure and biological activity. Food Chem. 128, 573–584. https://doi.org/10.1016/j.foodchem.2011.03.075.

Wolff, S.P., Dean, R.T., 1987. Glucose autoxidation and protein modification. The potential role of 'autoxidative glycosylation' in diabetes. Biochem. J. 245, 243–250. https://doi.org/10.1042/bj2450243.

Xie, Y., Van Der Fels-Klerx, H.J., Van Leeuwen, S.P.J., Fogliano, V., 2023. Occurrence of dietary advanced glycation end-products in commercial cow, goat and soy protein based infant formulas. Food Chem. 411, 135424 https://doi.org/10.1016/j.foodchem.2023.135424.

Yaylayan, V.A., 1997. Classification of the Maillard reaction: a conceptual approach. Trends Food Sci. Technol. 8, 13–18. https://doi.org/10.1016/S0924-2244(96)20013-5.

Zenker, H.E., van Lieshout, G.A.A., van Gool, M.P., Bragt, M.C.E., Hettinga, K.A., 2020. Lysine blockage of milk proteins in infant formula impairs overall protein digestibility and peptide release. Food Funct. 11, 358–369. https://doi.org/10.1039/C9FO02097G.

Zhang, H., Troise, A.D., Zhang, Hui, Fogliano, V., 2021. Cocoa melanoidins reduce the formation of dietary advanced glycation end-products in dairy mimicking system. Food Chem. 345, 128827 https://doi.org/10.1016/j.foodchem.2020.128827.

Zhang, H., Zhang, Hui, Troise, A.D., Fogliano, V., 2019a. Melanoidins from coffee, cocoa, and bread are able to scavenge α-dicarbonyl compounds under simulated physiological conditions. J. Agric. Food Chem. 67, 10921–10929. https://doi.org/10.1021/acs.jafc.9b03744.

Zhang, W., Poojary, M.M., Rauh, V., Ray, C.A., Olsen, K., Lund, M.N., 2019. Quantitation of α-dicarbonyls and advanced glycation endproducts in conventional and lactose-

hydrolyzed ultrahigh temperature milk during 1 Year of storage. J. Agric. Food Chem. 67, 12863–12874. https://doi.org/10.1021/acs.jafc.9b05037.

Zhao, D., Le, T.T., Larsen, L.B., Li, L., Qin, D., Su, G., Li, B., 2017. Effect of glycation derived from α-dicarbonyl compounds on the in vitro digestibility of β-casein and β-lactoglobulin: a model study with glyoxal, methylglyoxal and butanedione. Food Res. Int. 102, 313–322. https://doi.org/10.1016/j.foodres.2017.10.002.

Zhao, D., Sheng, B., Wu, Y., Li, H., Xu, D., Nian, Y., Mao, S., Li, C., Xu, X., Zhou, G., 2019. Comparison of free and bound advanced glycation end products in food: a review on the possible influence on human health. J. Agric. Food Chem. 67, 14007–14018. https://doi.org/10.1021/acs.jafc.9b05891.